From Molecular Complexes to Zwitterions and Final Products. Reactions between C_3O_2 and Amines

Bintou Sessouma,[†] Isabelle Couturier-Tamburelli,*[,†] Maurice Monnier,[†] Ming Wah Wong,[‡] Curt Wentrup,[§] and Jean Pierre Aycard[†]

Laboratoire de Physique des Interactions Ioniques et Moléculaires équipe de Spectrométrie et Dynamique Moléculaire UMR 6633, Université de Provence, F-13397 Marseille Cedex 20, France, Department of Chemistry, National University of Singapore, Kent Ridge, Singapore, Department of Chemistry, University of Queensland, Brisbane 4072, Queensland, Australia

Received: September 6, 2001; In Final Form: January 29, 2002

The formation of molecular complexes (prereactive intermediates) between C_3O_2 and amines (ammonia, dimethylamine, trimethylamine, and 4-(dimethylamino)pyridine) as well as the subsequent transformation of the complexes into C_3O_2−amine zwitterions in cryogenic matrixes (ca. 40 K) has been observed. In the case of dimethylamine, the formation of tetramethylmalonamide has also been documented. Calculations using density functional theory (B3LYP/6-31G(2d, p)) are used to assign all above species and are in excellent agreement with the IR spectra.

Introduction

In previous work, we have demonstrated the formation of molecular complexes between carbon suboxide, C_3O_2, and nucleophiles (water, ammonia, pyridine, and thiazole).[1−3] These complexes were generated by mixing the components together with a large excess of argon in the gas phase followed by matrix isolation at ca. 20 K. The resulting argon matrixes would typically contain a mixture of the unreacted components and the complexes. More of the complexes were formed on annealing the matrixes to ca. 40 K. Subsequently, the zwitterions were observable by IR spectroscopy at temperatures up to ca. 100 K or until all components of the matrixes evaporated.

It was shown in other work that ketenes react with pyridine at temperatures around 40 K to produce zwitterions.[1,4] If these two types of reaction are combined, it might be possible, under suitable experimental conditions, to monitor a chemical reaction from the initial formation of molecular van der Waals complex (prereactive intermediate[5]) to zwitterionic reactive intermediate and possibly on to final product (amides in the case of reaction with primary or secondary amines). This type of experiment has never been performed before.

Experimental Section

Pure C_3O_2 was synthesized using the method described by Miller et al.[6] Trimethylamine (TMA) was supplied by Fluka and used without further purification. Solid 4-(dimethylamino)-pyridine (DMAP) and solid malonamide were supplied by Aldrich. A gaseous mixture of DMAP/Ar was obtained by flowing argon over solid DMAP in the oven at −40 °C situated before the cryostat. NH_3 was supplied by Air Liquide. Dimethylamine (DMA) was supplied by Fluka. DMA is more reactive than the other amines and reacts with C_3O_2 in the gas phase. Therefore, a dual deposition system was constituted permitting simultaneous deposition of C_3O_2/Ar and DMA/Ar mixtures.

The gas mixtures were prepared by standard manometric techniques, or the appropriate solid sample was placed in the sublimation zone of a quartz oven tube (150 mm × 11 mm inner diameter which was attached to the vacuum sleeve of the cryostat) and sprayed on a gold-coated copper plate cooled at 20 K. The temperature of the oven (ca 900 °C) was monitored by two thermocouples. The sample was then gently sublimated with a continuous stream of argon being co-deposited on the observation plate. The deposition rate (2 mmol/h) of gas mixtures was controlled with an Air Liquide microleak (V.P/RX). A Fourier transform infrared spectrometer (Nicolet serie II 750) was used to record the spectra of samples cooled to 10 K in the range of 4000−550 cm^{-1} with a resolution of 0.12 cm^{-1}. The liquid spectrum was recorded on a Bruker IFS 25 spectrometer with a resolution of 2 cm^{-1}.

Kinetic studies of zwitterion formation were made by plotting the absolute absorbance variation as a function of time. Two temperatures were used for each zwitterion.

Results

1. Infrared Absorption Spectra of C_3O_2/TMA/Ar. *(a) C_3O_2/TMA/Ar.* The spectra recorded after co-depositing of C_3O_2/TMA/Ar (1/10/500) at 10 K show new absorption bands with respect to the spectra of pure $C_3O_{27a,b}$ and pure TMA[8] isolated in argon matrixes (Figure 1, Table 1). In the ν_{CCO} region between 2300 and 2100 cm^{-1}, the characteristic absorption bands of free C_3O_2 (ν_{CCOas} (asymmetric) = 2289 cm^{-1} and ν_{CCOs} (symmetric) = 2194 cm^{-1} for the most intense band of the several matrix sites) are observed. The most intense band of C_3O_2 in the presence of TMA appears at 2209 cm^{-1}. This value is shifted toward lower frequencies by 80 cm^{-1} with respect to the most intense ν_{CCOas} site. The ν_{CCOs} vibrational mode at 2189 cm^{-1} is only shifted toward lower frequencies by 5 cm^{-1}, but it sharply increases in intensity. The infrared spectrum of TMA remains essentially unchanged in the presence of C_3O_2. These observa-

* To whom correspondence should be addressed.
[†] Université de Provence.
[‡] National University of Singapore.
[§] University of Queensland.

10.1021/jp0134190 CCC: $22.00
Published on Web 04/06/2002

TABLE 1: Experimental and Calculated Frequencies (cm^{-1}) (B3LYP/6-31G(2d,p), Unscaled) in C_3O_2/TMA Complexes ($\Delta\nu = \nu(C_3O_2) - \nu$(Complexed))

C_3O_2 isolated (10 K)						complex (10 K)						$\Delta\nu$ ($\nu_{isolated}$-$\nu_{complex}$)		
expt (Ar)	I^a	expt (Xe)	I^a	calcd	I^a	expt (Ar)	I^a	expt (Xe)	I^a	calcd	I^a	expt (Ar)	expt (Xe)	calcd
2289	100.0	2271	100.0	2398	100.0	2209	100.0	2253	100.0	2318	100.0	80	18	80
2194	1.9	2188	2.4	2276	0.7	2189	4.3	2184	10.3	2262	3.8	5	4	14
1596	4.2	1588	6.3	1636	2.7					1582	0.8			
				816	0.1					895	0.7			
				577	0.0					593	0.0			
577	0.0			575	0.1					586	2.2			
539	0.2			565	2.7					584	2.1			
533	2.7			553	2.6					572	2.5			

[a] Integrated area for the experimental values and intensity for the calculated values in % relative to ν_{CCOas} of C_3O_2.

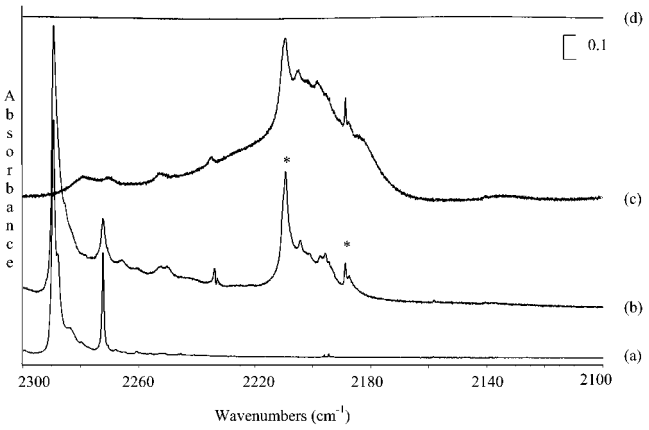

Figure 1. Infrared spectra of C_3O_2, TMA, and the C_3O_2/TMA complex isolated in Ar matrixes at 10 K in the 2300−2100 cm^{-1} region (ν_{CCO} symmetric and antisymmetric region). (a) C_3O_2/Ar in the ratio 1/500. (b) C_3O_2/TMA/Ar in the ratio 1/10/500. (c) C_3O_2/TMA/Ar in the ratio 1/10/500 at 10 K after 40 K. (d) TMA/Ar in the ratio 10/500. The complex bands are denoted by an asterisk.

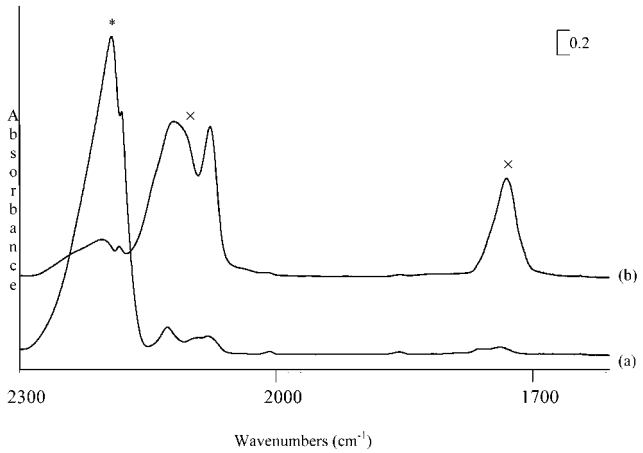

Figure 2. Infrared spectra of the solid C_3O_2/TMA complex at 45 K and the solid zwitterion C_3O_2/TMA at 70 K, (a) C_3O_2/TMA/Ar at 45K (argon evaporated), (b) Zwitterion C_3O_2/TMA at 70 K. The complex bands are denoted by an asterisk. The zwitterion band is denoted by a cross.

tions are analogous to those previous noted for NH_3 and pyridine.[1,2] The new bands are ascribed to the C_3O_2/TMA complex on the basis of the agreement with the theoretical calculated spectrum (Table 1).

(b) Annealing Experiments and Kinetics. To observe a reaction between C_3O_2 and TMA, the matrix obtained was warmed to 40 K (Figure 1). This operation causes C_3O_2 bands to decrease in conjunction with an increase in the ν_{CCOas} and ν_{CCOs} absorption bands of the C_3O_2/TMA complex. Warming results only in a reorganization of the trapping sites of the matrix and diffusion which yields more of the complex, but there is still very little amount of the zwitterion formed.

When the sample is warmed from 45 to 120 K after argon evaporation (Figure 2), the bands that are due to the solid complex decrease and completely disappear at 70 K. This is due to the formation of a zwitterion between C_3O_2 and TMA. Indeed, we observe the increase of three peaks at 2129, 2082, 1740, 916, and 673 cm^{-1} because of the emergence of the C_3O_2/TMA zwitterion (Table 2).

The kinetics of formation of the zwitterion can be described by the equation $A = A_0e^{-kt} + C$.[9] Figure 3 shows the decrease of the 2196 cm^{-1} solid complex band and the increase of the zwitterion band at 2129 cm^{-1} in the TMA matrix at 70 and 75 K during 1 h. On the basis of these two measurements, the activation energy is found to be ca. 63 kJ/mol.

(c) Other Matrixes and Experiments. Experiments using several other concentrations in argon (5/5/500 and 1/20/500, C_3O_2/TMA/Ar) were carried out in an effort to characterize the complex and the zwitterion. Pure C_3O_2−TMA matrixes were also formed at 45 K. In all these experiments, the same absorption bands appear corresponding to the C_3O_2/TMA complex. Subsequent warming of the C_3O_2−TMA matrixes to 130 K results in the formation of the absorption bands ascribed to the zwitterion (Table 2).

TABLE 2: Experimental and Calculated Frequencies (cm^{-1}) (B3LYP/6-31G(2d,p), Unscaled) of the C_3O_2/TMA Zwitterion ($\epsilon = 40$)

zwitterion					
expt (Ar host gs)	I^a	expt (Xe host gas)	I^a	calcd	I^a
2129−2082	100.0	2121−2084	100.0	2185	100.0
1740	29.8	1734	33.3	1893	24.9
994	0.4	993	1.8	1013	1.2
974	0.3	973	1.0	1004	0.8
916	1.9	919	4.4	913	3.4
797	0.4	798	1.8	802	0.9
785	0.2	786	2.0	706	0.2
673	0.8	679	1.6	640	16.7

[a] Integrated area for the experimental values and intensity for the calculated values in % relative to ν_{CCOas} of zwitterion.

A similar experiment was made at 30 K with xenon as matrix host with two different concentrations (1/10/500 and 1/20/500, C_3O_2/TMA/Xe). The spectrum recorded at 30 K shows two bands at 2253 and 2184 cm^{-1} attributed to the complex and shifted by 18 and 4 cm^{-1} respectively with regard to the C_3O_2 monomer bands (see the Supporting Information Figure S1, Table 1). At 90 K, the zwitterion appears at 2121, 2084, 1734, 919, and 679 cm^{-1} (see the Supporting Information Figure S2, Table 2).

2. Infrared Absorption Spectra of C_3O_2/DMAP/Ar. *(a) C_3O_2/DMAP/Ar.* As observed in the previous case, new absorp-

TABLE 3: Experimental and Calculated Frequencies (cm^{-1}) (B3LYP/6-31G(2d,p), Unscaled) in the C_3O_2/DMAP Complexes ($\Delta\nu = \nu(C_3O_2) - \nu$(Complexed))

C_3O_2 isolated (10 K)				Complex (10 K)				$\Delta\nu$ ($\nu_{isolated} - \nu_{complexe}$)	
expt	I^a	calcd	I^a	expt	I^a	calcd bent T_{Nu}	I^a	expt	calcd bent T_{Nu}
2289	100.0	2398	100.0	2241	100.0	2303	100.0	48	95
2194	1.9	2276	0.7	2193	3.7	2261	5.5	1	15
1596	4.2	1636	2.7	1595	37.0	1656	17.0	1	−20
577	0.0	575	0.1						
539	0.2	565	2.7						
533	2.7	553	2.6						

[a] Integrated area for the experimental values and intensity for the calculated values in % relative to ν_{CCOas} of C_3O_2.

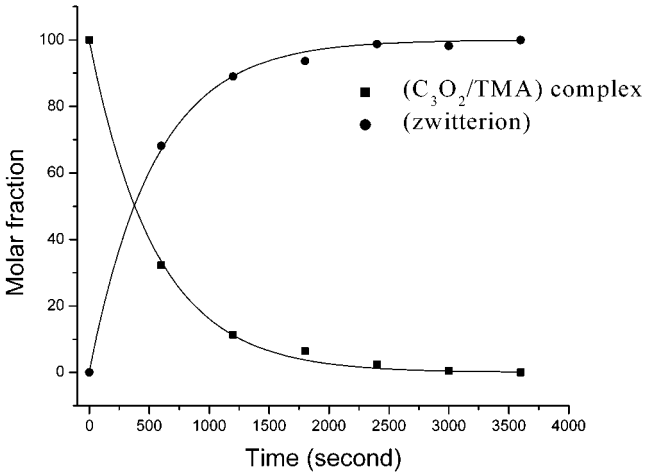

Figure 3. Decay of the C_3O_2/TMA complex and increase of the zwitterion during 1 h at 75 K, monitored by infrared spectroscopy at 2196 and 2129−2082 cm^{-1}.

TABLE 4: Experimental and Calculated Frequencies (cm^{-1}) (B3LYP/6-31G(2d,p), Unscaled) of the DMAP Zwitterion ($\epsilon = 40$)

zwitterion (90K)			
expt (Ar host gas)	I^a	calcd	I^a
2091−2071	100.0	2137	100.0
1696	18.7	1726	10.1
1640	18.3	1681	28.5
1035	26.8	1068	47.0
944	28.9	949	47.2

[a] Integrated area for the experimental values and intensity for the calculated values in % relative to ν_{CCOas} of zwitterion.

tion bands attributed to the complex with DMAP[10] appear in the infrared spectra recorded after co-depositing C_3O_2/DMAP/Ar at 10 K (Table 3). The three most intense bands at 2241, 2193, and 1595 cm^{-1}, assigned to ν_{CCOas}, ν_{CCOs}, and ν_{CCOas}, respectively, are shifted relative to those of pure C_3O_2 ($\Delta\nu_{CCOas} = 48$, $\Delta\nu_{CCOs} = 1$, and $\Delta\nu_{CCOas} = 1$ cm^{-1}). The infrared spectrum of DMAP remains unchanged in the presence of C_3O_2.

(b) Annealing Experiments. Annealing of the matrix to 40 K caused the complex bands to grow simultaneously with the disappearance of those due to C_3O_2 itself. Like in the TMA case, warming the C_3O_2−DMAP matrix (without argon) above 40 K caused disappearance of the solid complex (the most intense bad is situated at 2214 cm^{-1}) in concert with development of new bands at 2091, 2071, 1696, 1640, 944, and 697 cm^{-1} (Table 4, Figure 4). These absorption bands are assigned to the zwitterion (Table 4). Infrared monitoring of the reaction demonstrated that the complex disappeared at the same time as the new compound was formed. A kinetic study at two temperatures (90 and 95 K) yielded an activation energy of ca. 17 kJ/mol (Figure 5).

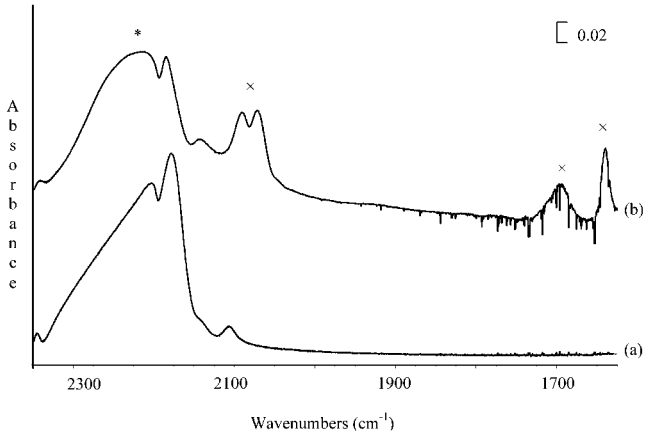

Figure 4. Infrared spectra of the solid C_3O_2/DMAP complex at 45 K and the solid zwitterion C_3O_2/DMAP at 90 K. (a) C_3O_2/DMAP/Ar at 45K (Ar evaporated). (b) Zwitterion C_3O_2/DMAP at 90 K. The complex band is denoted by an asterisk. The zwitterion bands are denoted by a cross.

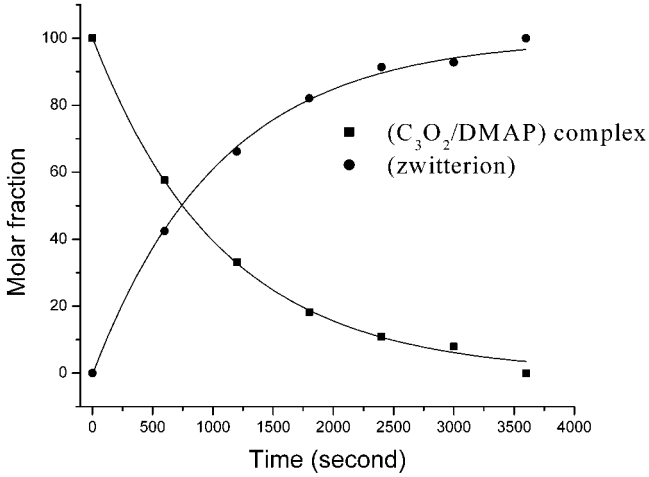

Figure 5. Decay of the DMAP absorption and increase of the zwitterion during 1 h at 90 K, monitored by infrared spectroscopy at 2214 and 2091−2071 cm^{-1}.

3. Infrared Absorption Spectra of C_3O_2/NH_3/Ar. *(a) C_3O_2/NH_3/Ar.* In a previous work,[1] we have reported on the C_3O_2/ammonia complex, which is the assumed prereactive intermediate en route to malonamide, formed by depositing a C_3O_2/NH_3/Ar mixture at 20−45 K. Because the pK_a of NH_3 (9.25) is close to those of TMA (9.8) and DMAP (9.6), NH_3 should also be able to form a zwitterion with C_3O_2.

(b) Annealing Experiment. The spectra recorded after co-deposition of C_3O_2/NH_3/Ar at 45 K show bands that are due to the solid complex (the most intense is situated at 2252 cm^{-1}). [1] Once the matrix was warmed, this band disappeared, and new strong absorptions at 2079 and 1636 cm^{-1} (Figure 6, Table 5),

TABLE 5: Experimental and Calculated Frequencies (cm^{-1}) (B3LYP/6-31G(2d,p), Unscaled) of the C_3O_2/NH_3 Complex[1] and Zwitterion ($\epsilon = 40$)

C_3O_2 (10 K)				complex (10 K)				$\Delta\nu$		zwitterion			
						calcd			calcd				
expt (Ar)	I^a	calcd	I^a	expt (Ar)	I^a	bent T_{Nu}	I^a	expt	bent T_{Nu}	expt	I^a	calcd	I^a
2289	100.0	2398	100.0	2222	100.0	2318	100.0	67	80	2079	100.0	2161	100.0
2194	1.9	2276	0.7	2191	18.0	2264	3.3	3	12	1636	62.9	1677	7.2
1596	4.2	1636	2.7										
577	0.0	575	0.1										
539	0.2	565	2.7										
533	2.7	553	2.6										

[a] Integrated area for the experimental values and intensity for the calculated values in % relative to ν_{CCOas} of C_3O_2 and zwitterion, respectively.

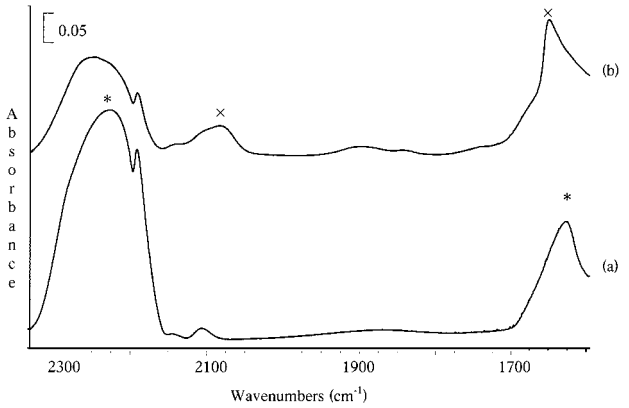

Figure 6. Infrared spectra of the solid C_3O_2/NH_3 complex at 45 K and the zwitterion C_3O_2/NH_3 at 95 K. (a) C_3O_2/NH_3/Ar at 45 K (Ar evaporated). (b) Zwitterion C_3O_2/NH_3 at 95 K. The complex bands are denoted by an asterisk. The zwitterion bands are denoted by a cross.

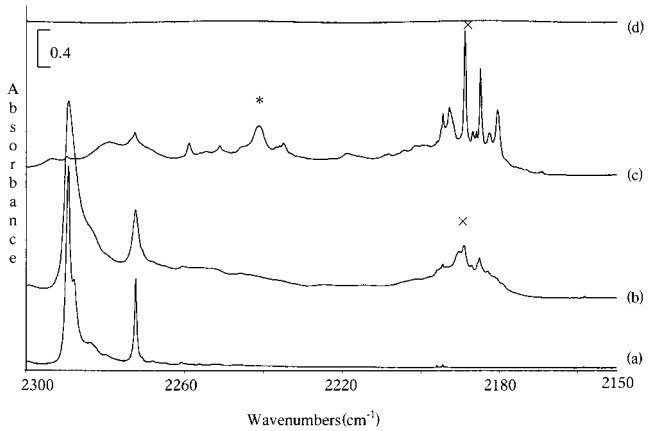

Figure 7. Infrared spectra of C_3O_2, DMA, and the C_3O_2/DMA zwitterion or methylenektene in the 2300−2150 cm^{-1}. (a) C_3O_2/Ar in the ratio 1/500. (b) C_3O_2/DMA/Ar 1/10/500. (c) C_3O_2/DMA/Ar in the ratio 1/10/500 at 10 K after 40 K. (d) DMA/Ar 10/500. The complex band is denoted by an asterisk. The zwitterion or methyleneketene band is denoted by a cross.

attributed to the zwitterion, appeared at 90−110 K. A kinetic study was made as in the previous cases. Constant monitoring of the reaction at 95 and 100 K demonstrated disappearance of the complex in concert with formation of the zwitterion (Figure 6, Table 5). The activation energy based on these two measurements was ca. 9 kJ/mol (see the Supporting Information Figure S3).

4. Infrared Absorption Spectra of C_3O_2/DMA/Ar. *(a) C_3O_2/DMA/Ar.* The DMA reacts with C_3O_2 in the gas phase when the two components are mixed. To avoid this reaction, separate mixtures of C_3O_2/Ar and DMA/Ar mixture were deposited simultaneously.

The spectra recorded at 10 K after co-depositing C_3O_2/Ar (1/250) and DMA/Ar (10/250) show weak absorption bands besides those that are due to C_3O_2 and DMA[12] (Figure 7). The more characteristic one in the argon matrix is at 2189 cm^{-1} and corresponds to a ketene function.

On the basis of the calculated IR spectra, these new bands may be attributed to either the zwitterion or the methyleneketene formed during the deposition (see Figure 8). Although the zwitterion is calculated to be unstable in the gas phase ($\epsilon = 1$), at this level of theory, it is stable in a polar medium ($\epsilon = 40$) and may form immediately on condensation of the reactants in the matrix. The methyleneketene is calculated to be more stable, but there is a high barrier toward its formation (Figure 8). It is not possible at present to make a clear distinction between these two species.

(b) Annealing Experiments. Warming the matrix to 40 K caused growth of the previous bands (zwitterion or methyleneketene) as well as emergence of new bands ascribed to the C_3O_2/DMA complex at 2241 cm^{-1} (Figure 7, Table 6). The band of the complex is assigned because of a good agreement with the calculated values (Table 6). The bands that are due to C_3O_2 and DMA decreased at the same time. The ν_{CCOas} band in the complex is shifted to lower frequencies by 48 cm^{-1} with respect to the C_3O_2 value.

A C_3O_2/DMA/Ar film was deposited at 45 K, but no new products bands were observed.

(c) Other Matrixes and Experiments. Like in the previous cases, several experiments with other concentrations in argon (5/5/500 and 1/20/500) were carried out in order to characterize the products of reaction and the complex. Pure DMA−C_3O_2 matrixes were obtained at 45 K after evaporation of argon. The bands ascribed to the C_3O_2/DMA zwitterion or methyleneketene and the complex were observed (Figure 9, Table 7).

Another peak is present at 2133 cm^{-1} that persists till 60 K (Figure 9, Table 7). From 40 K until 300 K, new peaks grow at 2935, 2879, 1633, 1553, 1390, and 1137 cm^{-1} (the most characteristic bands are shown in Figure 9, Table 8) corresponding to amide formation (Scheme 1). The 1636 cm^{-1} band persists until 300 K. To confirm the presence of the amide, ether followed by DMA were added to C_3O_2 cooled in liquid nitrogen. The mixture was transferred to a −100 °C bath and was warmed to room temperature. The amide was isolated and characterized by its IR spectrum (2925 and 1633 cm^{-1} in CH_2Cl_2).

Analogous experiments were performed using helium as a carrier gas (concentration 1/2/1000 and 1/20/200) with deposition at 10 K. The same product bands were observed, and they are listed in Table 6−8.

5. Theoretical Calculations. *(a) Geometries of Complexes: C_3O_2...TMA, C_3O_2..DMAP, and C_3O_2...DMA.* To establish the molecular structures and stabilities of the C_3O_2/amine complexes

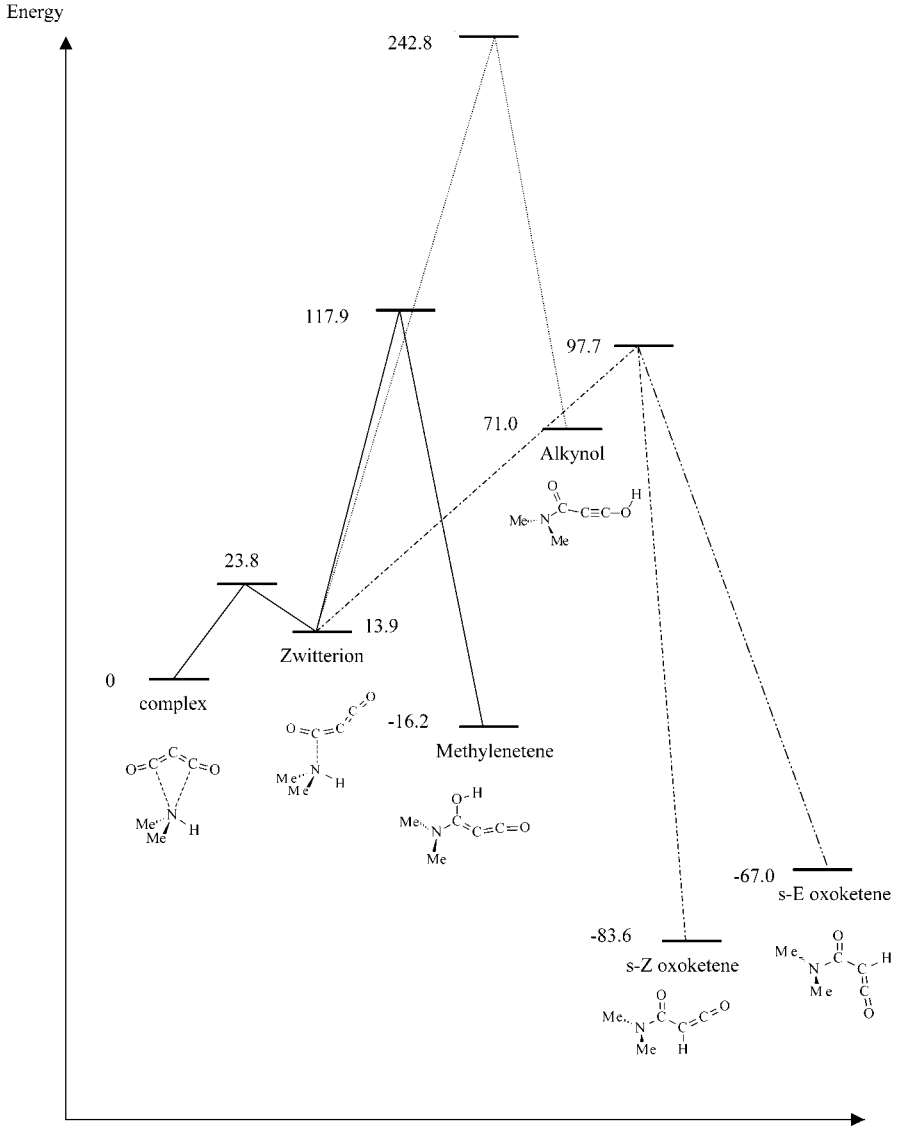

Figure 8. Calculated energy barriers (G3(MP2), in kJ mol^{-1}) between the C_3O_2/DMA zwitterion and the reaction product investigated: oxoketene, alkynol, and methylenketene.

TABLE 6: Experimental and Calculated Frequencies (cm^{-1}) (B3LYP/6-31G(2d,p), Unscaled) in C_3O_2/DMA Complexes ($\Delta\nu$ = $\nu(C_3O_2)$ − ν(Complexed))

C_3O_2 isolated (10 K)						complex (10 K)						$\Delta\nu$ ($\nu_{isolated}$-$\nu_{complexe}$)		
expt (Ar)	I^a	expt (He)	I^a	calcd	I^a	expt (Ar)	I^a	expt (He)	I^a	calcd bent T_{Nu}	I^a	expt (Ar)	expt (He)	calcd bent T_{Nu}
2289	100.0	2171	100.0	2398	100.0	2241	100.0	2236	100.0	2308	100.0	48	−65	90
2194	1.9	2199	4.8	2276	0.7	2193	3.4	2184	3.7	2262	4.3	1	15	14
1596	4.2			1636	2.7									
577	0.0			575	0.1									
536	0.2			565	2.7									
533	2.7			553	2.6									

*Integrated area for the experimental values and intensity for the calculated values in % relative to ν_{CCOas} of C_3O_2. This is not a He matrix but neat C_3O_2

and zwitterions, ab initio and density functional theory (DFT) calculations were carried out using the Gaussian 94 and 98 programs.[13] Geometry optimizations were carried out using the DFT B3LYP[14] method with the 6-31G(2d,p) basis set. Harmonic vibrational frequencies were determined at the optimized geometries and compared with experimental data (Tables 1−6). Higher-level relative energies were determined at the MP2/6-311+G(2d,p)//B3LYP/6-31G(2d,p) + ZPE level. The effects of a polar medium (dielectric constant $\epsilon = 40$) were examined by the self-consistent reaction field (SCRF) solvation method.[15] For the C_3O_2−DMA system, the structures and energies of various isomers in the gas phase were also investigated by the high-level G3(MP2) theory.[16]

Several geometric arrangements are possible for the van der Waals complex between the amine (pyridine) and C_3O_2 subunits. On the basis of our previous studies on the C_3O_2/NH_3 and C_3O_2/pyridine complexes,[1,2] the nitrogen atom of the amine or pyridine is expected to attack carbon suboxide on the C_α atom of the ketene moiety. In our theoretical study of the C_3O_2/pyridine complex,[2] we found two plausible structures, with the C_3O_2

TABLE 7: Experimental and Calculated Frequencies cm^{-1} (B3LYP/6-31G(2d, p)) of C_3O_2/DMA Zwitterion, Methylketene, s−*E*-Oxoketene, s−*Z*-Oxoketene, and Alkynol

product (90 K)								zwitterion			methylene ketene		s−*E*-oxo ketene		s−*Z*-oxo ketene		alkynol	
expt (Ar host gas)	I^b	expt (He host gas)	I^b	product (45 K)[a] expt	I^b	expt	I^b	calculated unscaled	scaled[c]	I^b	calcd scaled[c]	I^b	calcd scaled[c]	I^b	calcd scaled[c]	I^b	calcd scaled[c]	I^b
2148−2120−2088	100.0	2147−2122−2087	48.5	2133	100.0	2132	100.0	2167	2080	100.0	2102	100.0	2114	100.0	2122	100.0	2273	100.0
1644	26.6	1642	28.0					1860	1786	26.7	1653	28.0	1650	59.3	1623	26.8	1637	59.3
											1510	7.6	1480	5.8	1476	9.1	1489	7.8
								677	650	14.3	1401	6.3	1353	25.3	1374	24.4	1373	31.6
											1281	7.8	1147	16.5	1098	18.4	1192	29.2
											1073	17.0	1069	10.4			1049	57.8
773	3.7	733	2.9								669	0.6	742	2.1	715	2.4	1039	29.4
																	910	6.9
																	708	2.7

[a] Direct deposition at 45 K (cf. Figure 15). [b] Integrated area for the experimental values and intensity for the calculatedd values in % relative to ν_{CCOas} of C_3O_2. [c] Scaled by 0.96.

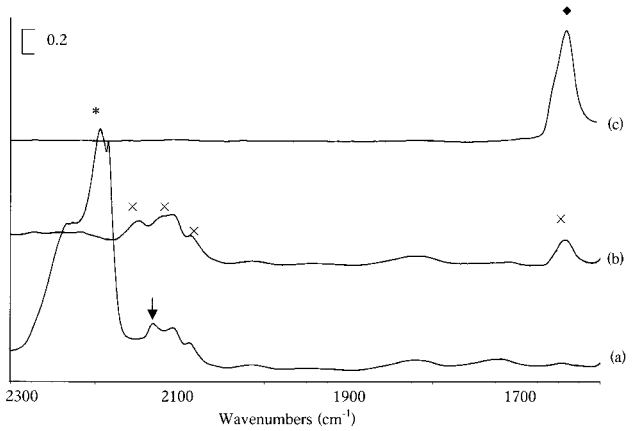

Figure 9. Infrared spectra of the solid C_3O_2/DMA complex at 45 K and intermediate product (zwitterion or methylenketene) C_3O_2/DMA at 90 K in the 2300−1600 region. (a) C_3O_2/DMA/Ar at 45 K (Ar evaporated). (b) Zwitterion C_3O_2/DMA or methyleneketne at 90 K. (c) C_3O_2/DMA at 130 K. The complex band is denoted by an asterisk. The intermediate product bands (zwitterion or methyleneketene) are denoted by a cross. The band at 2133 cm^{-1} is denoted by an arrow. The *N*,*N*,*N*′,*N*′-tetramethylmalonamide band is denoted by ♦.

TABLE 8: Experimental and Calculated Frequencies cm^{-1} (B3LYP/6-31G(2d,p), Scaled by 0.96) *N*,*N*,*N*′,*N*′-tetramethylmalonamide

product (130 K)				calcd	
expt (Ar)	I^a	expt (He)	I^a	calcd	I^a
2935	13.0	2933	15.4	2899	20.3
2879	8.9	2877	8.7	2885	15.8
1636	100.0	1631	100.0	1659	100.0
1553	10.2	1551	9.3	1491	2.3
1498	5.5	1501	4.9	1486	6.3
1390	15.4	1395	15.3	1367	30.8
1262	2.9	1267	3.4	1246	10.8
1137	11.1	1138	11.3	1137	21.7
1059	2.1	1060	1.8	1070	3.4

[a] Integrated area for the experimental values and intensity for the calculatedd values in % relative to ν_{CCOas} of C_3O_2.

moiety in either a bent or a linear form (cf. Scheme 2). For the various systems examined in this paper, the existence of the bent and linear complexes depends on both the level of theory and the basis set employed. For instance, both bent and linear forms of C_3O_2/DMA complexes can be located on the MP2/6-31G* potential energy surface. However, only the bent complex exists at the HF/6-31G* level, and the bent form is the only stable equilibrium structure at the B3LYP/6-31G* level. Most importantly, we found that a proper description of the bent

SCHEME 1: Reaction of Formation of *N*,*N*,*N*′,*N*′-tetramethylmalonamide

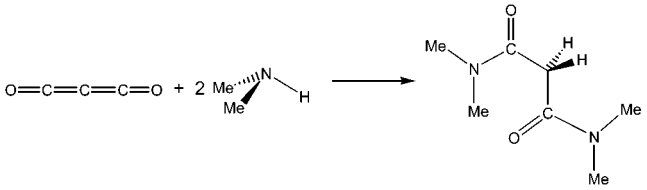

SCHEME 2: Two Types of C_3O_2/Amine van der Waals Complexes Considered

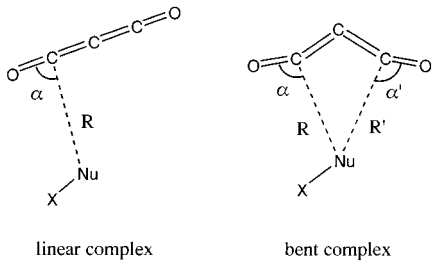

linear complex bent complex

complex requires a second set of d polarization functions. Hence, we have used the 6-31G(2d,p) basis set for our DFT optimizations and frequency calculations. The relative stability between the bent and linear forms of the C_3O_2/DMA complex is confirmed by higher-level calculations at the MP2 and B3LYP levels with the larger 6-311+G(2df,p) basis set. At these higher levels of theory, the bent form is the preferred structure of the van der Waals complex. The existence of the bent C_3O_2···amine complexes demonstrates that the energy gained from two favorable N···C_α donor−acceptor interactions is sufficient to overcome the energy required to bend the C_3O_2 subunit. The CCC bond angle in the bent complex corresponds to a change of hybridization of the central carbon atom from sp to sp^2. In the case of the C_3O_2/DMAP complex, several other possible geometrical arrangements were also considered, but they are calculated to be higher in energy (see the Supporting Information).

The bent C_3O_2/amine complexes are characterized by two sets of independent variables *R* (*R*′) and α (α′) (Scheme 2), denoting the distance between the amine (pyridine) nitrogen atom and C_α of carbon suboxide and the intermolecular angle between R and the CO moiety of carbon suboxide, respectively. The *R* and *R*′ values (3.15−3.52 Å) are typical of van der Waals complexes. For the C_3O_2−DMAP system with a C_{2v} symmetry, the two sets of *R* (*R*′) and α (α′) values are identical. However, these parameters are found to be different for other complexes.

In the C_3O_2/NH_3 complex, one of the N···C_α distances is shorter than the other by 0.22 Å. This suggests that there is significant interaction between the O and H atoms. As with the C_3O_2/pyridine complex[2], the CH···O interaction may play an important role in governing the structures of the C_3O_2/DMA and C_3O_2/TMA complexes.

The calculations provide insight into the stability and spectroscopic properties of the C_3O_2/amine complexes. The optimized geometries of the complexes ($\epsilon = 1$) and zwitterions ($\epsilon = 40$) are given in Scheme 3. Complexation affects the geometry of the partner molecules and their most significant stretching frequencies. Several key calculated structural parameters and the vibrational frequencies for the complexed molecules are summarized in Scheme 3 and Tables 1, 3, and 6, respectively. The CCC moieties in these complexes are strongly bent. Interestingly, the calculated CCC angles are quite similar, 135−140°. Accordingly, the C═C bonds are lengthened in the complexes. The bending of the C_3O_2 subunit leads to significant changes in the CCO stretching vibrations of the complex: an increase of the antisymmetric frequency and an increase of the IR intensity of the symmetric vibration. To identify the nature of the complexes presents in argon matrixes, it is appropriate to compare the experimental C_3O_2 frequency shifts in the complexes with those calculated by the DFT method. Examination of these data (Tables 1, 3, and 6) shows reasonably good agreement between the experimental and calculated frequency shifts for the bent complexes. In all cases, the calculated frequency shift of the antisymmetric CCO stretching mode is in good agreement with experimental value. It is important to note that the corresponding calculated frequency shift in the linear complex is very small, thus indicating that the observed C_3O_2/amine complexes have a bent C_3O_2 moiety.

The calculated complexation energies of the various systems examined in this paper are given in Table 9. In the isolated state ($\epsilon = 1$), the binding energies of the bent complexes are in the range of 10−21 kJ mol^{-1}, with the calculated order of stability (NH_3 < DMA < TMA < DMAP) in accord with the electron donating ability of the amines. On the basis of the natural bond orbital (NBO) analysis,[14] the degree of charge transfer is small (0.006−0.009) in all cases. On going from the gas phase to a polar medium, there are small changes on the structures and stabilities of all of the complexes (Table 9).

(b) Mechanism of Zwitterion Formation. Except for the C_3O_2−DMAP system, a zwitterionic type of structure does not exist on the gas-phase ($\epsilon = 1$) potential energy surface. However, a stable equilibrium structure can be located in a dielectric medium of $\epsilon = 40$. In the case of the C_3O_2−NH_3 system, the solvation effect of the zwitterion by ammonia was modeled by including two NH_3 molecules, which are hydrogen bonded to two hydrogens, in the SCRF calculation. All of the zwitterions have a planar structure and are characterized by a somewhat long N−C bond, ranging from 1.48 to 1.73 Å (Scheme 3). The C_3O_2 subunits in the complex are transformed into C═C═O and C═O functional groups in the zwitterion. As a consequence, the characteristic frequencies of the latter are significantly different from those of the van der Waals complexes. As indicated by their large dipole moments (>10 D) and charge distributions, the zwitterions are best described as charge-transfer species. Hence, they are strongly stabilized in the presence of a polar medium. The stabilty of the zwitterion correlates with the N−C bond distance. In particular, DMAP forms a stable zwitterion with C_3O_2 even in the gas phase. On going from the gas phase to a polar medium, the N−C bond length of this zwitterion reduces significantly from 1.63 to 1.48

SCHEME 3: Optimized Geometries (B3LYP/6-31G(2d,p)) of C_3O_2/Amine (amine = NH_3, DMA, TMA, and DMAP) Complexes and Zwitterions

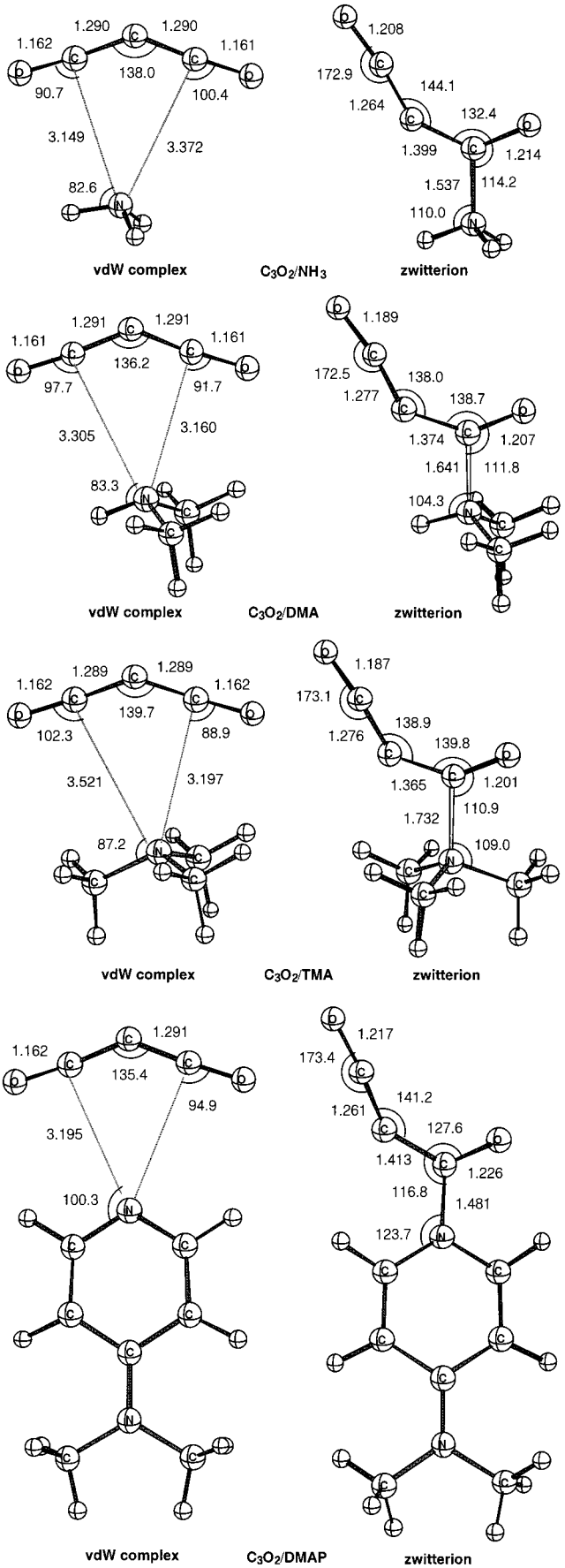

TABLE 9: Calculated Energies (kJ mol^{-1}) of Different Complexes and Zwitterions at the MP2/6-311+G(2d,p)// B3LYP/6-31G(2d,p) + ZPVE Level in Comparison of the Monomer Energy

	binding energy of complex		zwitterion[a]
species	$\epsilon = 1$	$\epsilon = 40$	$\epsilon = 40$
C_3O_2/NH_3	−10.0	8.1	*b*
C_3O_2/DMA	−15.9	−16.8	0.2
C_3O_2/TMA	−18.6	−18.9	2.2
C_3O_2/DMAP	−20.8	−23.8	−78.6[c]

[a] Relative energy of the zwitterion with respect to the van der Waals complex. [b] The C_3O_2/NH_3 zwitterion is not calculated to bea stable species in a dielectric medium of $\epsilon = 40$. [c] The C_3O_2/DMAP has a stable zwitterion structure in the gas phase ($\epsilon = 1$, +37.0 kJ mol^{-1} higher in energy than the complex).

Å. A dramatic medium effect is also seen in the C=O stretching frequency, which undergoes a red shift of 149 cm^{-1}. The calculated DFT frequencies of this system for $\epsilon = 40$ are in very good agreement with the observed values (Table 4). This illustrates the importance of incorporating a solvent reaction field in calculating the structures and stabilities of these charge-transfer type species.

For the aliphatic amines (DMA and TMA), the zwitterions are predicted to be close in energy to the van der Waals complexes in a polar medium (Table 9). In distinct contrast, the zwitterion of the C_3O_2/DMAP system is 79 kJ mol^{-1} more stable than the corresponding bent complex! At the same level of theory, the zwitterion and bent complex of the C_3O_2−pyridine system are calculated to have similar energies (7 kJ mol^{-1}). It thus appears that the *p*-dimethylamino substituent on pyridine has a dramatic effect on stabilizing the zwitterionic structure, as is also observed in its reaction with dipivaloylketene.[18] A similar finding has been reported for other ketene−pyridine complexes.[19,20] It is important to note that the DFT theory grossly underestimates the binding energies of the complexes and relative stabilities of the zwitterions. On the other hand, relative energies predicted at the MP2 level of theory are in significantly better agreement compared to those obtained at the higher-level of theory (e.g., G3(MP2)).

(c) Reaction's Products of DMA and C_3O_2. For the C_3O_2−DMA system, we have examined the reaction profile for the interconversion of the complex and various plausible addition products, namely oxoketene, alkynol and methylketene, at the G3(MP2) level of theory (Figure 8). The most characteristic frequencies of these compounds are presented in Table 7. The calculated activation barriers between the zwitterion and the different isomers are summarized in Figure 8. There is good agreement between the observed peak at 2133 cm^{-1} and the calculated frequency of the oxoketene after scaling by a factor of 0.96 (Table 7). For the band obtained at 90 K (2148, 2120, 2088, and 1644 cm^{-1}), it is very difficult to differentiate between the zwitterion and the methyleneketene. *N,N,N′,N′*-tetramethylmalonamide frequencies have also been calculated and are very close to those of the final product (Table 8).

6. Discussion and Conclusion

The annealing experiments indicate that TMA and C_3O_2 react in the matrix above 40 K to form a molecular complex. Some of this complex was already formed during the deposition of the gaseous mixture. These observations are analogous to those made previously with ammonia, thiazole, and pyridine.[1−3] On further warming, the bands due to the complex start to disappear again at ca. 45 K and have completely vanished at 70 K. The new species formed is assigned to the zwitterion (2129, 2082, 1742, 916, and 672 cm^{-1}). This species is stable till 120 K when the solid evaporates.

Similarly, DMAP and C_3O_2 form a complex (2241 cm^{-1}) which is transformed into a zwitterion (2091 cm^{-1}) above 40 K. The zwitterion is observable till 190 K. These results are different from those obtained with the less basic molecules pyridine and thiazole,[2,3] where only the complexes were detectable. These results are in line with the finding that the zwitterions formed from ketenes and DMAP and much more stable than those derived from ketenes and pyridine.[4,18]

Although the transformation of the solid C_3O_2/ammonia complex (2252 cm^{-1}) into zwitterion (2079 cm^{-1}) was not previously investigated,[1] we have now found that this reaction also takes place at ca. 90 K.

DMA also forms a complex (2241 cm^{-1}) during deposition. DMA is so reactive that it is necessary to perform a dual deposition and then avoid extensive reaction between C_3O_2 and DMA in the gas phase. In an argon matrix, the complex increases in intensity till ca. 40 K and is easily transformed into the product of reaction ((methyleneketene or zwitterion) 2189 cm^{-1}). The intensity of this intermediates species increases till 60 K, then decreases, and finally disappears at 190 K. The relative amounts of complex, intermediate, and free C_3O_2 obtained in the initial matrix depend on the concentrations of the starting material in Ar or He. The rate of the transformation of the complex into the intermediate is also dependent on the relative concentrations, i.e., on the amounts of free amine available for reaction.

For the tertiary amines such as TMA and DMAP, a proton-transfer mechanism leading to the amide reaction product is not possible, and the reactions have to stop at the zwitterion stage. In the case of DMA, proton transfer is possible, and the amide product is observed. This is formed after the formation of van der Waals complexes and zwitterionic or methylenketene intermediates.

In the case of DMA, the solid DMA/C_3O_2 zwitterion or methyleneketene intermediate (2148, 2120, and 2088 cm^{-1}) starts to disappear at temperatures above 90 K. New bands in the ketene region increase in intensity when this intermediate decreases, but these bands also eventually vanish when the temperature is increased. Various reaction products, namely, alkynol, methylenketene, and oxoketene, have been investigated theoretically (Figure 8). The G3(MP2) calculations indicate that the alkynol is unstable relative to the zwitterion and complex, and it is not therefore considered as a likely product. The attribution of the 2133 cm^{-1} band to the s−Z oxoketene is not unequivocal but is made considering the stability of this compound (83.6 kJ mol^{-1} below DMA/C_3O_2). New bands also appear in the carbonyl region, in particular the band at 1641 cm^{-1}, which continues to grow when all of the ketene species have disappeared. It is therefore associated with the final product of the reaction, the *N,N,N′,N′*-tetramethylmalonamide.

The transformation kinetics of the complexes of NH_3, TMA, and DMAP into zwitterions followed pseudo-first-order rate laws for ca. 40% of the reaction, indicating that the complexes do not isomerize directly to the zwitterions in unimolecular reactions but that exchange with an amine molecule from the surrounding medium is involved. Evidence for similar reactions in solution has been reported by Sung and Tidwell[21] and Raspoet et al.;[22] a second amine molecule was shown to be involved in the amination of ketenes. Complex reactions with an order ≥ 2 was made evident in further work.[15,22−23]

Our detailed kinetic analysis reveals a one to one correspondence between the disappearance of complexes and the

appearance of the C_3O_2−amine zwitterion formed upon nucleophilic addition.

The pseudo first-order kinetics fit the experimental results. Nevertheless, our results do not consider the inhomogeneity[24] of the medium, and therefore they can only give indicative energy barriers. Nevertheless, the experimental values are in satisfactory agreement with the calculated barriers.

Acknowledgment. The CNRS is gratefully acknowledged for its financial support.

Supporting Information Available: Scheme 4 showing the several other possible optimized geometrical arrangements (B3LYP/6-31G(2d,p)) of C_3O_2/DMAP complexes and zwitterions (1 page). Figure S1 showing the infrared spectra of C_3O_2, TMA, and the C_3O_2/TMA complex in Xe matrixes at 30K in the 2300−2160 cm^{-1} region (1 page). Figure S2 showing the infrared spectra of the C_3O_2/TMA complex at 45 K and the C_3O_2/TMA zwitterion at 90 K after Xe evaporation (1 page). Figure S3 showing the decay of NH_3 absortion and increase of zwitterion during 1 h at 95 K (1 page). This infromation is available free of charge via the Internet at http://pubs.acs.org.

References and Notes

(1) (a) Couturier-Tamburelli, I.; Chiavassa, T.; Aycard, J. P. *J. Am. Chem. Soc*. **1999**, *121*, 3756. (b) Couturier-Tamburelli, I. Ph.D. Thesis, Université de Provence, Provence, France, 1998.

(2) Couturier-Tamburelli, I.; Aycard, J. P.; Wong, M. W.; Wentrup, C. *J. Phys. Chem. A.* **2000**, *104*, 3466.

(3) Couturier-Tamburelli, I.; Sessouma, B.; Aycard, J. P. *J. Mol. Struct.* **2001**, *560*, 197.

(4) (a) Qiao, G. G.; Andraos, J.; Wentrup, C. *J. Am. Chem. Soc.* **1996**, *118*, 5634. (b) Visser, P.; Zuhse, R.; Wong, M. W.; Wentrup, C. *J. Am. Chem. Soc.* **1996**, *118*, 12598.

(5) Legon, A. C. *J. Chem. Soc., Chem. Commun.* **1996**, *109*.

(6) Miller, F. A.; Fateley, W. G. *Spectrochim. Acta* **1964**, *20*, 253.

(7) (a) Piétri, N.; Chiavassa, T.; Allouche, A.; Aycard, J. P. *J. Phys. Chem. A* **1997**, *101*, 1093. (b) Piétri, N. Ph.D. Thesis, Université de Provence, Provence, France, 1996.

(8) Golfarb, T. D.; Khare, B. N. *J. Chem. Phys*. **1967**, *46*, 3379.

(9) Siebrand, W.; Wildman, T. A. *Acc. Chem. Res*. **1986**, *19*, 238.

(10) Gupta, S. P.; Ahmad, S.; Goel, R. K. *Indian J. Phys. B* **1987**, *61*, 427.

(11) Schiavoni, M. M.; Mack, H. G.; Ulic, S. E.; Della Vecoda, C. A. *Spectrochim. Acta Part A* **2000**, *56*, 1553.

(12) Wentrup, C.; Rao, R. V. V.; Frank, W.; Fulloon, B. E.; Moloney, D. W. J.; Mosland, T. *J. Org. Chem.* **1999**, 3608.

(13) Frisch, M. J.; Trucks, G. W.; Schlegel, H. B.; Scuseria, G. E.; Robb, M. A.; Cheeseman, J. R.; Zakrzewski, V. G.; Montgomery, J. A., Jr.; Stratmann, R. E.; Burant, J. C.; Dapprich, S.; Millam, J. M.; Daniels, A. D.; Kudin, K. N.; Strain, M. C.; Farkas, O.; Tomasi, J.; Barone, V.; Cossi, M.; Cammi, R.; Mennucci, B.; Pomelli, C.; Adamo, C.; Clifford, S.; Ochterski, J.; Petersson, G. A.; Ayala, P. Y.; Cui, Q.; Morokuma, K.; Malick, D. K.; Rabuck, A. D.; Raghavachari, K.; Foresman, J. B.; Cioslowski, J.; Ortiz, J. V.; Stefanov, B. B.; Liu, G.; Liashenko, A.; Piskorz, P.; Komaromi, I.; Gomperts, R.; Martin, R. L.; Fox, D. J.; Keith, T.; Al-Laham, M. A.; Peng, C. Y.; Nanayakkara, A.; Gonzalez, C.; Challacombe, M.; Gill, P. M. W.; Johnson, B. G.; Chen, W.; Wong, M. W.; Andres, J. L.; Head-Gordon, M.; Replogle, E. S.; Pople, J. A. *Gaussian 98*; Gaussian, Inc.: Pittsburgh, PA, 1998.

(14) (a) Becke, A. D. *J. Chem. Phys*. **1993**, *98*, 5648. (b) Lee, C. W.; Yang, W.; Parr, R. G. *Phys. Rev. B* **1988**, *37*, 785.

(15) (a) Wong, M. W.; Frisch, M. J.; Wiberg, K. B. *J. Am. Chem. Soc*. **1991**, *113*, 4776. (b) Wong, M. W.; Wiberg, K. B.; Frisch, M. J. *J. Chem. Phys*. **1991**, *95*, 8991.

(16) Curtiss, L. A.; Raghavachari, K.; Trucks, G. W.; Pople, J. A. *J. Chem. Phys.* **1991**, *94*, 7221.

(17) Reed, A. E.; Curtiss, L. A.; Weinhold, F. *Chem. Rev.* **1988**, *88*, 899.

(18) Kollenz, G.; Holzer, S.; Kappe, C. O.; Dalvi, T. S.; Fabian, W. M. F.; Sterk, H.; Wong, M. W.; Wentrup, C. *Eur. J. Org. Chem.* **2001**, 1315.

(19) Gompper, R.; Wolf, U. *Liebigs Ann. Chem*. **1979**, 1388.

(20) Wong, M. W. *J. Org. Chem*. Submitted for publication.

(21) Sung, K.; Tidwell, T. T. *J. Am. Chem. Soc*. **1998**, *120*, 3043.

(22) Raspoet, G.; Nguyen, M. T.; Kelly, S.; Hegarty A. F. *J. Org. Chem.* **1998**, *63*, 9669.

(23) Allen, A. D.; Tidwell, T. T. *J. Org. Chem*. **1999**, *64*, 266.

(24) Andraos, J. *J. Phys. Chem. A* **2000**, *104*, 1532.